

Lifetime of the lowest 0^+ , $T = 1$ state of ^{22}Na B. T. Neyer,* D. L. Clark,[†] J. S. Dunham,[‡] W. A. Seale,[§] J. L. Thornton,**
R. T. Westervelt, and S. S. Hanna*Department of Physics, Stanford University, Stanford, California 94305*

B. A. Brown

National Superconducting Cyclotron Laboratory, Michigan State University, East Lansing, Michigan 48824

B. H. Wildenthal

Department of Physics and Atmospheric Science, Drexel University, Philadelphia, Pennsylvania 19104

(Received 17 November 1986)

The lifetime of the lowest 0^+ , $T = 1$ state of ^{22}Na , which decays 100% to a lower 1^+ , $T = 0$ state, has been measured by the recoil-into-plunger Doppler method. The result, $\tau = 29.3 \pm 1.0$ ps, gives the average $\tau = 28.3 \pm 0.8$ ps when combined with an earlier result. A comparison of the $B(M1)$ extracted from this lifetime with the Gamow-Teller strength for the analog β decay from the ground state of ^{22}Mg to the same 1^+ , $T = 0$ state in ^{22}Na shows that the orbital part of the $M1$ γ transition is greatly enhanced relative to the spin part. These results are interpreted in the context of realistic shell-model calculations for sd -shell nuclei.

We report the measurement of the lifetime of the second excited state of ^{22}Na . This 0^+ , $T = 1$ state at 657 keV decays to the 1^+ , $T = 0$ state at 583 keV by an $M1$ transition. Thus, the transition is the isobar analog of the Gamow-Teller (GT) β decay of the 0^+ , $T = 1$ ground state of ^{22}Mg to the same 583 keV ^{22}Na state. Since the $M1$ transition involves both spin and orbital angular momentum and the β decay involves only spin, a comparison of the two transition rates allows one to determine the importance of the orbital angular momentum in the $M1$ transition.

The recoil-into-plunger Doppler method, which is suited to the expected lifetime range, was used to measure the lifetime. The plunger (stopper) apparatus has been described earlier.¹ The reaction $^{19}\text{F}(\alpha, n)^{22}\text{Na}$ was used to produce the state. The target consisted of $100 \mu\text{g}/\text{cm}^2$ of CaF_2 evaporated onto a tightly stretched $1.1 \text{ mg}/\text{cm}^2$ Ni foil. A good reaction yield was obtained at a beam energy of 4.3 MeV, which was equivalent to 3.7 MeV at the target layer after passage through the Ni foil. This energy is low enough to prevent feeding of the 0^+ state from higher levels. A "singles" experiment was possible for this reaction because the negative Q value of the reaction and the low beam energy ensured that the nuclei recoiled in a narrow forward cone.

Because the 657 keV state decays 100% to the 583 keV state, the only gamma ray available for the lifetime measurement has the low energy of 74 keV. Hence we used a lithium drifted silicon, Si(Li), detector. This provided much better energy resolution (less than 0.5 keV) than a Ge(Li) detector (over 1 keV) and good efficiency for low energy γ rays. Since the recoil velocity in this experiment was less than 1% of the speed of light, the better energy resolution of the Si(Li) detector, which was mounted at 0° , was crucial to the experiment. Data were accumulated in the usual way, the plunger being moved in steps of 4–12

μm , with the larger steps taken at the larger target-to-stopper distances.

In a normal plunger experiment, the stopped and Doppler-shifted peaks are separated and it is then a simple matter to determine the number of counts in each of these peaks. However, because of the low energy of the gamma ray and the small Doppler shift in this experiment the stopped and shifted peaks could not be visually resolved. Nevertheless, the resolution in the γ -ray energy spectra still was sufficient to allow determination of each peak's intensity.

One approach to determining these intensities is to use

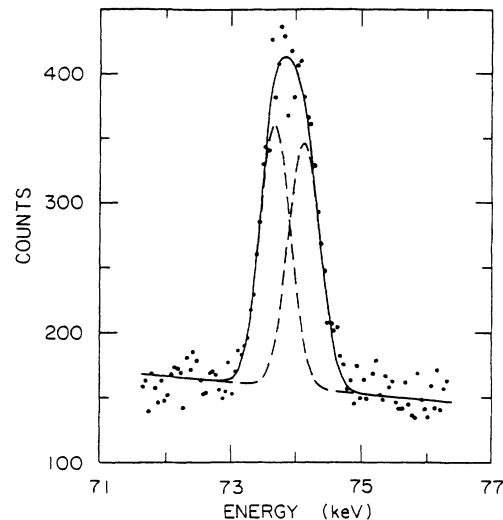


FIG. 1. Two-line fit to ^{22}Na spectrum with stopper set at a distance of $33 \mu\text{m}$ corresponding to a time of 18 ps. As is apparent, the distance corresponds to approximately one half-life.

the centroid method, since it is possible to relate the centroid energy of the unresolved peak to the ratio of the counts in the stopped and shifted peaks. Fifield *et al.*² used this method on peaks obtained with a Ge(Li) detector to measure the lifetime of this state. However, this method has the disadvantage that any small unmonitored gain shift present in the experiment could lead thereby to an incorrect lifetime. To correct for such shifts in our work, both the 197 and 109 keV transitions produced in ^{19}F by α bombardment, as well as the 32.1 keV line of a ^{137}Cs source, were monitored. Oscillations in the centroids of magnitudes 0.05–0.1% with periods of approximately 24 h were observed in all three of these calibration peaks. The centroid shifts were corrected for these gain changes. However, this procedure increases the uncertainty of the measurement.

To overcome this uncertainty we also employed an alternate technique to determine the intensities. We took advantage of the better resolution of the Si(Li) detector and fitted each spectrum with a combination of two overlapping Gaussian peaks and a background curve to obtain the counts in the stopped and shifted peaks. The parameters of the Gaussian curves were obtained by summing all the data to obtain good statistics and fitting the summed data with two Gaussians plus background. The parameters that gave the best χ^2 fit were selected for the analysis of the individual measurements. A typical fit is shown in Fig. 1.

The numbers of counts in the stopped and shifted peaks, N_0 and N_S , respectively, were used to compute the ratio $R = N_0/(N_0 + N_S)$ for each target-to-stopper distance D . These values were then fitted to the equation given by Jones *et al.*³

$$R = e^{-D/V\tau} \left[1 + \alpha_2(D/V\tau) \frac{\Delta^2}{3} + \alpha_4(D/V\tau) \frac{\Delta^4}{5} \right], \quad (1)$$

where τ is the mean life, V the average forward com-

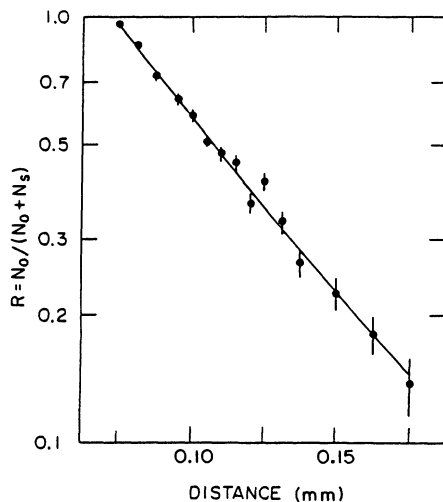


FIG. 2. Ratio of counts from stopped nuclei to total counts as a function of stopper distance. The solid curve is a least squares fit of Eq. (1).

ponent of the velocity, and Δ the spread in velocity; the functions α_2 and α_4 represent slowly varying functions which have magnitudes of the order unity. The velocity spread Δ is known from kinematics to be in the range 0.3–0.6% of c . Fitting the data with Δ varying from 0.0% to 0.6% resulted in lifetime values consistent to $\pm 2\%$. Fitting the final data with Δ free, as shown in Fig. 2, resulted in the value of $\tau = 29.3 \pm 1.0$ ps. Corrections were applied to account for the finite size of the detector in determining the recoil velocity and for the changes in detector efficiency. The value obtained is in agreement with the value of 27.1 ± 1.2 ps measured by Fifield *et al.*² Combining the two measurements yields the value 28.3 ± 0.8 ps.

This value of the lifetime of the $J^\pi = 0^+$, $T=1 \rightarrow J^\pi = 1^+$, $T=0$, 657 keV \rightarrow 583 keV transition in ^{22}Na yields a value of $B(M1) = 49.7 \pm 0.14 \mu_N^2$. The experimental $\log ft$ value⁴ for the corresponding Gamow-Teller β decay of the analog of the 0^+ state, the ground state of ^{22}Mg , to the same 1^+ level yields a value of $B(\text{GT}) = 1.38 \pm 0.04$.⁵ The implications of these experimental values for the nuclear structures of the two states and for the general properties of $M1$ and Gamow-Teller transitions can be discussed in the context of predictions of realistic shell-model calculations. In Table I we present the experimental values and several sets of corresponding theoretical values. All of these predictions are based on the complete $d_{5/2}-s_{1/2}-d_{3/2}$ model wave functions obtained by diagonalizing the effective Hamiltonian described in Ref. 6. This Hamiltonian has been shown⁶ to generate wave functions which give a generally good accounting of nuclear properties throughout the sd shell.

The initial predictions shown in Table I are obtained by using these wave functions to evaluate the matrix elements of the “free nucleon” $M1$ and Gamow-Teller operators. The coupling constants in these operators are taken from the magnetic moments of the free neutron and proton and the lifetime of the free neutron, respectively. These “free nucleon” predictions are appreciably larger than experiment in each case, with the theoretical/experimental ratio for the Gamow-Teller

TABLE I. Experimental $B(M1)$ and $B(\text{GT})$ values of the $0^+, 1 \rightarrow 1^+, 0$ transitions for $A=22$ compared with various theoretical values. The experimental $B(M1)$ value is the average of this and one previous work (Ref. 2).

	$B(M1)$ $0^+ \rightarrow 1^+$	$B(\text{GT})$ $0^+ \rightarrow 1^+$
Experiment	4.97(14)	1.38(04)
Free nucleon operators	7.54	2.96
Towner and Khanna renormalizations ^a	6.91	2.12
Brown and Wildenthal renormalizations ^b	6.56	1.81
Brown and Wildenthal renormalizations ^b with remixed wave functions	5.15	1.29

^aBased on an interpolation of the effective single-particle matrix elements calculated by Towner and Khanna (Ref. 10) for $A=17$ and 39.

^bBased on the effective single-particle matrix elements obtained from fits to moments (Ref. 8) and GT β decay (Ref. 5).

values being significantly larger than that for the $M1$ values. These results are consistent with the relationships between measured Gamow-Teller and $M1$ strengths and the predictions of this family of wave functions for other sd -shell nuclei.

A survey⁵ of all Gamow-Teller data in the sd shell indicates that experimental strengths are approximately 0.60 as large as those predicted with a free-nucleon normalization for the operator. There is considerable evidence from (p,n) reaction experiments that this “quenching” of experimental strength is a universal phenomenon in complex nuclei.⁷ Studies of $M1$ data in the sd shell^{8,9} do not reveal a need for such a simple renormalization of the magnetic dipole operator as the global quenching found for Gamow-Teller transitions. However, the $M1$ operator is more complex than the Gamow-Teller operator, because of the presence of the orbital as well as the intrinsic angular momentum term. A renormalization of the $M1$ operator clearly improves the absolute agreement between experiment and the present shell-model theory and in the typical case this renormalization also reduces the predicted strength.

The renormalization of shell-model operators is a corollary of the highly truncated basis which must be employed even in relatively realistic, complete-major-shell, calculations such as those of Ref. 6. The “free nucleon” forms of the operators must be corrected for the effects of truncating the nucleon configuration space to a few shell-model orbitals and for ignoring mesonic and nucleon-excitation degrees of freedom entirely. A particularly complete set of predictions of these renormalizations for $M1$ and Gamow-Teller operators in light nuclei has been given in Ref. 10. The second set of predictions in Table I is obtained by using the same shell-model amplitudes and the effective operators of Ref. 10, as formulated in the A -dependent averages of Ref. 8. These “effective-operator” predictions are closer to the experimental values than the “free-nucleon” predictions by significant amounts, but they are still too large.

The third theoretical entries in Table I are obtained by again using the same shell-model amplitudes of Ref. 6, this time to evaluate the matrix elements of effective $M1$ and Gamow-Teller operators empirically determined in Refs. 8 and 5 by analyses of large sets of sd -shell data. These empirical analogs of the effective operators theoretically derived in Ref. 10 yield slightly smaller strengths still, but theory is still appreciably larger than experiment in both cases. These remaining discrepancies must be attributed to the shell-model wave functions for the particular states involved in this transition.

In the simple jj -coupling limit of the shell model, the lowest 0^+ , $T=1$, state of $A=22$ would have a wave function consisting of $(d_{5/2})^6$ with seniority equal to zero. This 0^+ , $T=1$ configuration is connected by the spin and orbital angular momentum operators to $T=0$ configurations characterized by $(d_{5/2})^5$, seniority equal to two, and $(d_{5/2})^5(d_{3/2})^1$. In the actual configuration-mixed wave functions used in the present calculations these simple components are heavily mixed with other sd -shell configurations. The lowest 0^+ , $T=1$ state is dominated by the $(d_{5/2})^6$ component but fragments of the two $T=0$ com-

ponents noted above which connect to it are widely distributed.

The Gamow-Teller data suggest that the failure of the present wave functions in predicting too large strengths for the transition of interest here is correlated with their predicting transition strengths which are too small to the second 1^+ , $T=0$ level.⁵ It appears that the components of the 1^+ wave functions which yield $M1$ and Gamow-Teller strengths are slightly misdistributed, so that the lower state has too much and the upper state too little strength. This type of defect, in which the total amount of strength predicted for two adjacent levels of the same spin is roughly correct but the predicted ratio between the levels is incorrect, is the most common problem with shell-model calculations of the present type.

This hypothesis can be tested by generating slightly “rotated” shell-model wave functions in which the amplitudes of the two adjacent levels are mixed according to

$$|1_1^+\rangle' = a |1_1^+\rangle + b |1_2^+\rangle$$

and

$$|1_2^+\rangle' = b |1_1^+\rangle - a |1_2^+\rangle.$$

When the first two 1^+ , $T=0$ levels calculated for ^{22}Na with the Hamiltonian of Ref. 5 are mixed so as to generate the experimentally observed ratio of Gamow-Teller strength to these two levels, the values of a and b are 0.987 and 0.154, respectively. These remixed wave functions, together with the empirically renormalized operators of Refs. 5 and 8, are used to obtain the final theoretical estimates in Table I. The mixing amplitudes fixed by the Gamow-Teller strength ratio suffice to yield $M1$ and Gamow-Teller strengths for the lowest 1^+ , $T=0$ state which agree with experiment.

The free-nucleon isovector g factor is an order of magnitude larger than the orbital g factor. It is hence expected that the spin component of the $M1$ operator dominates $M1$ strengths. The renormalizations of the $M1$ operator reduce the spin coefficient and enhance the orbital coefficient,^{8,10} but the qualitative dominance of spin is unchanged. Under the assumption of specific values for the g factors and the Gamow-Teller coupling constant, the strengths of analog $M1$ and Gamow-Teller transitions can be combined to yield a value for the ratio of the orbital and spin matrix elements.¹¹ With the free-nucleon operators this relationship is given by

$$B(M1) = 1.88(1 + 0.106\langle l \rangle / \langle s \rangle)^2 B(GT).$$

The experimental values of Table I yield the values of $\langle l \rangle / \langle s \rangle = 3.60 \pm 0.18$ and -22.5 ± 0.18 . This exceptional dominance of orbital over spin, while atypical of the general run of $M1$ phenomena, is not unique.

Similar situations have been reported for the $A=9$ and 20 systems,^{11,12} for example. It is also not unexpected in the context of the shell-model wave functions. Many $M1$ transitions between low-lying levels in light sd -shell systems are predicted to have dominant orbital ($d_{5/2} \rightarrow d_{5/2}$) components. The transition treated in this work is one such example. The strengths predicted from the free-

nucleon operators yield a ratio of 1.55, while the final, "remixed" wave functions, together with the empirical operators, yield detailed agreement with the data and hence agreement as well with the ratio of $\langle l \rangle / \langle s \rangle$ extracted from them.

This work was supported in part by the U.S. National Science Foundation, Grants PHY83-10044, PHY86-10124, PHY83-12245, and PHY85-09736, and by Fundação de Amparo a Pesquisa do Estado de São Paulo (FAPESP), Universidade de São Paulo, São Paulo, Brazil.

*Present address: Monsanto Mound Research Corp., Mound Facility, Mound Rd, Miamisburg, OH 45342.

†Present address: Research and Engineering, Eastman Kodak Co., 901 Elmgrove Rd., Rochester, NY 14650.

‡Present address: Physics Department, Middlebury College, Middlebury, VT 05753.

§On leave from Instituto de Física, Universidade de São Paulo, São Paulo, Brazil.

**Present address: Schlumberger Well Services, 5000 Gulf Freeway, Houston, TX 77252.

¹D. L. Clark, H. T. King, J. R. Hall, and S. S. Hanna, Stanford University, Nuclear Laboratory Progress report, 1979, p. 127 (unpublished).

²L. K. Fifield, A. R. Poletti, and D. C. Radford, *J. Phys. G* **6**, 723 (1980).

³K. W. Jones, A. Z. Schwarzschild, E. K. Warburton, and D. B. Fossan, *Phys. Rev.* **178**, 1773 (1969).

⁴P. M. Endt and C. Van der Leun, *Nucl. Phys.* **A310**, 1 (1978).

⁵B. A. Brown and B. H. Wildenthal, *At. Data Nucl. Data*

Tables **33**, 347 (1985).

⁶B. H. Wildenthal, in *Progress in Particle and Nuclear Physics*, edited by D. H. Wilkinson (Pergamon, Oxford, 1984), Vol. 11, p. 5.

⁷See, e.g., C. D. Goodman and S. D. Bloom, in *Proceedings of the International Conference on Spin Excitations in Nuclei*, Telluride, Colorado, 1982, edited by F. Petrovich, G. E. Brown, G. Garvey, C. D. Goodman, R. A. Lindgren, and W. G. Love (Plenum, New York, 1984).

⁸B. A. Brown and B. H. Wildenthal, *Phys. Rev. C* **28**, 2397 (1983).

⁹B. H. Wildenthal, private communication.

¹⁰I. S. Towner and F. C. Khanna, *Nucl. Phys.* **A399**, 334 (1983).

¹¹S. S. Hanna, in *Isospin in Nuclear Physics*, edited by D. H. Wilkinson (North-Holland, Amsterdam, 1969), p. 591.

¹²C. J. Martoff, J. A. Bistirlich, K. M. Crowe, M. Koike, J. P. Miller, S. S. Rosenblum, W. A. Zajc, H. W. Baer, A. H. Wapstra, G. Strassner, and P. Truöl, *Phys. Rev. Lett.* **46**, 891 (1981).